Navigating Explanatory Multiverse Through Counterfactual Path Geometry

Kacper Sokol † 12 Edward Small † 1 Yueqing Xuan † 1

Abstract

Counterfactual explanations are the de facto standard when tasked with interpreting decisions of (opaque) predictive models. Their generation is often subject to algorithmic and domain-specific constraints - such as density-based feasibility for the former and attribute (im)mutability or directionality of change for the latter - that aim to maximise their real-life utility. In addition to desiderata with respect to the counterfactual instance itself, the existence of a viable path connecting it with the factual data point, known as algorithmic recourse, has become an important technical consideration. While both of these requirements ensure that the steps of the journey as well as its destination are admissible, current literature neglects the multiplicity of such counterfactual paths. To address this shortcoming we introduce the novel concept of explanatory multiverse that encompasses all the possible counterfactual journeys and shows how to navigate, reason about and compare the geometry of these paths – their affinity, branching, divergence and possible future convergence – with two methods: vector spaces and graphs. Implementing this (interactive) explanatory process grants explainees more agency by allowing them to select counterfactuals based on the properties of the journey leading to them in addition to their absolute differences.

1. Indistinguishability of Counterfactual Paths

Counterfactuals are some of the most popular explanations when faced with unintelligible machine learning models (ML). Their appeal – both to lay and technical audiences – is grounded in decades of social science research [Miller, 2019] and compliance with various legal

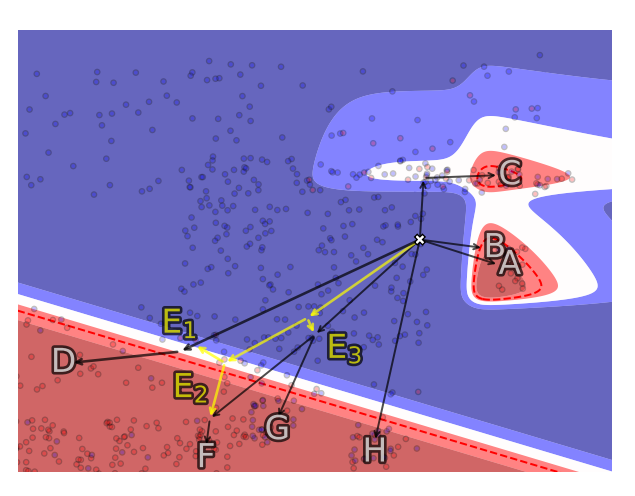


Figure 1: Example of **explanatory multiverse** constructed for tabular data with two continuous (numerical) features. It shows various types of **counterfactual path geometry** – their *affinity*, *branching*, *divergence* and *convergence*. Each journey terminates in a (possibly the same or similar) counterfactual explanation but characteristics of the steps leading there make some explanations more attractive targets, e.g., by giving the explainee more agency through multiple actionable choices towards the end of a path.

frameworks [Wachter et al., 2017]. Fundamentally, counterfactual explanation generation relies on finding an instance whose class is opposite to the factual data point while minimising the distance between the two – a retrieval process that can be tweaked and tuned to satisfy bespoke desiderata.

The increasing popularity of counterfactuals and their flexible generation mechanism have encouraged researchers to incorporate sophisticated technical and social requirements into their retrieval algorithms to better reflect their real-life situatedness. Relevant technical aspects include tweaking a minimal number of attributes to guarantee their sparsity, or ensuring that they come from a data manifold either by relying on hitherto observed instances [Keane & Smyth, 2020; Poyiadzi et al., 2020; van Looveren & Klaise, 2021] or by constructing them in dense regions [Förster et al., 2021]. Desired social properties reflect real-life constraints embedded in the underlying operational context and data domain, e.g., (im)mutability of certain features, such as date of birth, and directionality of change of others, such as age.

[†]Equal contribution. ¹ARC Centre of Excellence for Automated Decision-Making and Society, School of Computing Technologies, RMIT University, Australia ²Department of Computer Science, ETH Zurich, Switzerland. Correspondence to: Kacper Sokol kacper.sokol@inf.ethz.ch, Edward Small kacper.sokol@inf.ethz.ch, Edward Small kacper.sokol@inf.ethz.ch, Edward Small kacper.sokol@inf.ethz.ch, Yueqing Xuan yueqing.xuan@student.rmit.edu.au, Yueqing Xuan yueqing.xuan@student.rmit.edu.au.

The mechanisms employed to retrieve these explanations have evolved accordingly: from techniques that simply output counterfactual instances [Wachter et al., 2017; Russell, 2019; Romashov et al., 2022] (accounting for selected social and technical desiderata as part of optimisation), to methods that construct viable paths between factual and counterfactual points [Poyiadzi et al., 2020; Downs et al., 2020; Förster et al., 2021; Karimi et al., 2021], ensuring feasibility of this journey (called *algorithmic recourse* [Ustun et al., 2019]).

All of these properties aid in generating admissible counterfactuals, but they do not offer guidance on how to discriminate between them. Available explainers tend to output multiple counterfactuals whose differences, as it stands, can only be captured through high-level desiderata (e.g., chronology and coherence), quantitative metrics (e.g., completeness, proximity and neighbourhood density) or qualitative assessment (e.g., user trust and confidence) [Sokol & Flach, 2020a; Keane et al., 2021; Small et al., 2023]. In principle, explanation plurality is desirable since it facilitates (interactive) personalisation by offering versatile sets of actions to be taken by the explainees instead of just the most optimal collection of steps (according to a predefined objective), thus catering to unique needs and expectations of diverse audiences [Sokol & Flach, 2018; 2020c]. Nonetheless, this multiplicity is also problematic as without incorporating domain-specific knowledge, collecting user input or relying on generic "goodness" heuristics and criteria [Keane et al., 2021] to prune the explanations – which remains an open challenge – we are likely to overwhelm the explainees.

While comparing the counterfactual data points themselves – e.g., based on minimal similarity, maximal diversity as well as their overall feasibility and actionability - may inform their pruning, considering the (geometric) relation between the paths leading to them could prove more powerful. Current literature treats such paths as independent, thus forgoing any spatial relation between them, whether captured by their direction, length or number of steps (including alignment and size thereof). Additionally, while the feasibility of attribute tweaks (i.e., feature actionability or mutability) is often considered, their directionality and magnitude have been largely neglected; e.g., age can only increase at a fixed rate. Modelling such aspects of counterfactual paths is bound to offer domain-independent, spatially-informed heuristics that reduce the number of explanations for users to consider, grant them more agency, enable informed decision-making and support forward planning.

The role of geometry in (counterfactual) explainability is captured by Figure 1, which demonstrates the diverse characteristics of counterfactual paths for a two-dimensional toy data set with continuous numerical features. When considered in *isolation*, these paths have the following properties:

B is short but terminates close to a decision boundary, thus

- carries high uncertainty;
- A while longer and leading to a high-confidence region, it lacks data along its journey, which signals that it may be infeasible;
- C addresses the shortcomings of A, but it terminates in an area of high instability (compared to D, E_i, F, G & H);
- **G & H** also do not exhibit the deficiencies of A, but they lead to an area with a high error rate;
- **D** & F have all the desired properties, but they require the most travel; and

 E_i are feasible, but they are *incomplete* by themselves.

While such considerations have become commonplace in the literature, they treat each destination and path leading to it independently, thus forgoing the benefit of accounting for their spatial relation such as affinity, branching, divergence or convergence. For example, while accessing D, F & G via E_i elongates the journey leading to these counterfactuals – thus making them less attractive based on current desiderata – it maximises explainee agency by providing multiple recourse choices along the trajectory.

Reasoning about the properties of and comparing counter-factual paths is intuitive in two-dimensional spaces – as demonstrated by Figure 1 – but doing so in higher dimensions requires a more principled approach. To this end, we formalise the concept of *explanatory multiverse* (Section 2), which embraces the multiplicity of counterfactual explanations and captures the *geometry* (i.e., spatial dependence) of journeys leading to them. Our conceptualisation accounts for technical, *spatially-unaware*, desiderata prevalent in the literature – e.g., plausibility, path length, number of steps, sparsity, magnitude of attribute change and feature actionability – and defines novel, *spatially-aware*, properties such as branching delay, branching factor, (change in) path directionality and affinity between journeys. We propose two possible approaches to embrace explanatory multiverse:

- 1. vector-based paths, which can rely on data density (model-agnostic) or gradient methods, and are apt for continuous feature spaces (Section 3); and
- 2. pathfinding in (directed) graphs, which can be built for data based on a predefined distance metric, and is best suited for discrete feature spaces (Section 4).

In addition to imbuing counterfactuals with spatial awareness, explanatory multiverse reduces the number of admissible explanations by *collapsing* paths based on their affinity and *ranking* them through our spatially-aware desiderata. We make it easy for others to embark on this novel counterfactuals research journey by releasing a Python package that implements our methods, which we call FACELIFT¹.

¹github.com/xuanxuanxuan-git/facelift

From the explainees' perspective, our approach helps them to navigate explanatory multiverse and grants them more initiative and agency, thus empowering meaningful exploration, customisation and personalisation of counterfactuals. For example, by choosing a path recommended based on a high number of diverse explanations accessible along it – refer to segments E_i in Figure 1 – the user is given numerous opportunities to receive the desired outcome while enacting a consistent set of changes, thus reducing the number of u-turns and backtracking arising in the process. Explanatory multiverse is also compatible with human-in-the-loop, interactive explainability [Sokol & Flach, 2018; 2020c; Keenan & Sokol, 2023] and a relatively recent decision-support model of explainability, which relies on co-construction of explanations and complements the more ubiquitous "prediction justification" paradigm [Miller, 2023]. We explore and discuss these concepts further in Section 5, before concluding the paper and outlining future work in Section 6.

2. Preliminaries

Before we formalise explanatory multiverse desiderata (Section 2.2), we summarise the notation (Section 2.1) used to introduce our two methods. Throughout this paper we assume that we are given a (state-of-the-art) explainer that generates counterfactuals along with steps leading to them, such as FACE [Poyiadzi et al., 2020] or any algorithmic recourse technique [Ustun et al., 2019; Karimi et al., 2021]. The proposed solutions work with explainers that follow actual data instances and those that operate directly on feature spaces (e.g., by using the density of data distribution).

2.1. Notation

We denote the m-dimensional input space as \mathcal{X} , with the explained (factual) instance given by \mathring{x} and the explanation (counterfactual) data point by \check{x} . These instances are considered in relation to a predictive model $f: \mathcal{X} \mapsto \mathcal{Y}$, where \mathcal{Y} is the space of possible classes; therefore, $f(\mathring{x}) \neq f(\check{x})$ and the prediction of the former data point $f(\mathring{x}) = \mathring{y} \in \mathcal{Y}$ is less desirable than of the latter $f(\check{x}) = \check{y} \in \mathcal{Y}$. Vector p-norms, which provide a measurement of length, are defined as $\|v\|_p = (\sum_{i=1}^n |v_i|^p)^{\frac{1}{p}}$. Distance functions are denoted by $s: \mathcal{X} \times \mathcal{X} \mapsto \mathbb{R}$, where the score of 0 represents identical instances, i.e., $s(x_a, x_b) = 0 \implies x_a \equiv x_b$, and the higher the score, the more different the data points are.

To discover \check{x} and the *steps* necessary to transform \mathring{x} into this instance, we apply a state-of-the-art, path-based explainer – see Section 2.2 for the properties expected of it – that generates (multiple) counterfactuals along with their journeys. Each such explanation $Z^{[k]}$ is represented by an $m \times n$ matrix whose n columns $z_i^{[k]} \in \mathcal{X}$ capture the sequence of steps in the m-dimensional input space,

i.e., $Z^{[k]} = [z_1^{[k]} \cdots z_n^{[k]}]$, such that if we start at the factual point \mathring{x} , we end at the counterfactual instance \check{x} like so: $\check{x} = \mathring{x} + \sum_{i=1}^n z_i^{[k]}$. For the **vector-based** explanatory multiverse, each step can be discounted by a weight factor w_i that captures its properties, with the weight vector $w = [w_1 \cdots w_n]$ adhering to $||w||_2 = 1$ and $w_1 \geq w_2 \geq \cdots \geq w_{n-1} \geq w_n$.

For the **graph-based** approach, we take G=(V,E) to be a (directed) graph with vertices V and arcs (directed edges) E. Each vertex $v_i \in V$ corresponds to a data point $x_i \in \mathcal{X}$ in the input space; these are connected with (directed) edges $e_{i,j} \in E$ that leave v_i and enter v_j . Assuming that v_i represents the explained instance \mathring{x} , thus the starting point of a path, and v_j is the target counterfactual data point \check{x} , thus where the journey terminates, we can identify multiple paths $Z^{[k]}$ connecting them. Here, the columns $z_i^{[k]}$ of the $m \times n$ matrix $Z^{[k]}$ representing an n-step explanatory journey hold a sequence of vertices v_i along this path, i.e., $z_i^{[k]} \equiv v_i$, with $z_1^{[k]} \equiv \mathring{x}$ and $z_n^{[k]} \equiv \check{x}$. Such a journey can also be denoted by the corresponding sequence of edges $E_{i,j} = [e_{i,a}, \ldots, e_{b,j}] \subseteq E$. In this case, the edges may encode weight factors w_i that capture properties of each transition (akin to the vector space).

2.2. Desiderata

By using pre-existing state-of-the-art path-based explainers, we can retrieve counterfactuals according to the well-known, spatially-unaware desiderata that account for the notions of: (1) distance between the explained instance and the explanation [Wachter et al., 2017; Tolomei et al., 2017]; (2) feature (im)mutability or actionability [Ustun et al., 2019; Karimi et al., 2021]; (3) feasibility of the data point used as the counterfactual [Pawelczyk et al., 2020; Poyiadzi et al., 2020; Downs et al., 2020; van Looveren & Klaise, 2021]; and (4) representativeness of the resulting explanations [Mothilal et al., 2020; Keane et al., 2021].

The first group includes properties such as counterfactual path length, its number of steps, number of features being tweaked as well as *magnitude* of these individual changes, striving for smallest distance and minimal number of affected features, i.e., similarity or closeness, and parsimony. The second set accounts for (domain-specific) constraints pertaining to feature alterations; specifically, (im)mutability of attributes, direction and rate of their change as well as their actionability from a user's perspective (e.g., some tweaks are irreversible, some can be enacted by explainees and others – mutable but non-actionable – are properties of the environment). The third category deals with characteristics of counterfactual data points (as well as the intermediate instances that constitute their paths); in particular, we expect them to be feasible according to the underlying data distribution - thus come from the data manifold, enforced either through density constraints or by following pre-existing instances – and of *high confidence*, i.e., robust, in view of the predictive model being explained. The fourth group, which is the least explored, deals with *multiplicity* of admissible counterfactual explanations; primarily, these are *path-agnostic* objectives that attempt to select a subset of counterfactuals that are the *most diverse* and *least similar*.

We embed our conceptualisation of *explanatory multiverse* on top of these properties – which it inherits by relying on state-of-the-art, path-based counterfactual explainers – and extend them with three novel, *spatially-aware* desiderata.

Agency captures the number of choices – leading to *diverse* counterfactuals – available to explainees as they traverse explanatory paths. High agency offers a selection of explanations and stimulates *user initiative*. It can be measured as a *branching factor*, i.e., the number of paths leading to representative explanations accessible at any given step.

Loss of Opportunity encompasses the *incompatibility* of subsets of explanations that emerges as a consequence of enacting changes prescribed by steps along counterfactual paths. For example, moving towards one explanation may require backtracking the steps taken thus far – which may be impossible due to the directionality of feature change – to arrive at a different, equally suitable, counterfactual. This *cost of opportunity* can be measured by (a decrease in) the proportion of counterfactuals reachable after taking a step without the need of backtracking, which can be quantified by the degree of change in *path directionality* (vectors) or *vertex inaccessibility* (graphs).

Choice Complexity encapsulates the influence of explainees' decisions to follow specific counterfactual paths on the availability of diverse explanations. It can be understood as *loss of opportunity* accumulated along different explanatory journeys. For example, among otherwise equivalent paths, following those whose *branching is delayed* reduces early commitment to a particular set of explanations. It can be measured by the distance (or number of steps and their magnitude) between the factual data point and the earliest consequential point of *counterfactual path divergence*.

To illustrate the benefits of navigating counterfactuals through the lens of explanatory multiverse, consider a patient who can receive a number of medical treatments. Choosing one of them may preclude others, e.g., due to drug incompatibility – a scenario captured by *loss of opportunity*. Deciding on medical procedures that are the most universal, thus shared across many therapies, allows to delay the funnelling towards specific courses of treatment – a benefit of accounting for *choice complexity*. In general, the

landscape of available treatments can be more easily navigated by taking actions that do not limit explainees' choices – a prime example of *agency*. Notably, we can strive for all of these desiderata simultaneously, weighting some in favour of others if necessary, which we explore in Section 5.

3. Vector Space Interpretation

It should be clear by now that outputting each admissible counterfactual as an independent sequence of steps and ordering these explanations based on their overall length is problematic on multiple levels. Accounting for their geometry helps to reduce their number shown to explainees and allows to rank them, but such an approach comes with challenges of its own.

3.1. Comparing Journeys of Varying Length

Counterfactual paths may differ in their overall length, number of steps or individual magnitude thereof, e.g., because of the data manifold shape. For example, juxtapose paths B and F in Figure 1, where the former is built with fewer steps and is much shorter than the latter. Comparing their geometry via their original components is thus infeasible as we could only do so up to the number of steps of the shorter of the two paths (assuming that these steps themselves are of similar length). We address this challenge by comparing counterfactual journeys through their relative sections.

Given two paths $Z^{[a]} \in \mathbb{R}^{m \times n_1}$ and $Z^{[b]} \in \mathbb{R}^{m \times n_2}$ differing in number of steps, i.e., $n_1 \neq n_2$, we encode them with an equal number of vectors p such that $\bar{Z}^{[a]}, \bar{Z}^{[b]} \in \mathbb{R}^{m \times p}$ are normalised journeys. To this end, we define a function

$$c_L(Z) = \sum_{i=1}^n ||z_i||_2$$
,

which provides us with the total length of a counterfactual path $Z \in \mathbb{R}^{m \times n}$ by summing the magnitude of its individual steps. We then select the number of steps p into which we partition each journey – these serve as comparison points for paths of differing length. Therefore, the j^{th} step of a normalised counterfactual journey $\bar{Z}^{[a]}$, $\bar{z}^{[a]}_{i}$, is

$$\bar{z}_{j}^{[a]} = \sum_{i=1}^{n_{1}} \delta_{z_{i}^{[a]}} \left(\frac{j}{p} c_{L}(Z^{[a]}) - \sum_{l=1}^{i} \|z_{l}^{[a]}\|_{2} \right) z_{i}^{[a]}$$

where

$$\delta_{z_i}(\zeta) = \begin{cases} 0 & \text{if } \zeta \leq 0 \\ \frac{\zeta}{\|z_i\|_2} & \text{if } 0 < \zeta \leq \|z_i\|_2 \\ 1 & \text{otherwise} \end{cases},$$

thus allowing for direct comparison with the corresponding step of the normalised path $\bar{Z}^{[b]}$. This procedure is captured by Algorithm 1 and demonstrated in Figure 2.

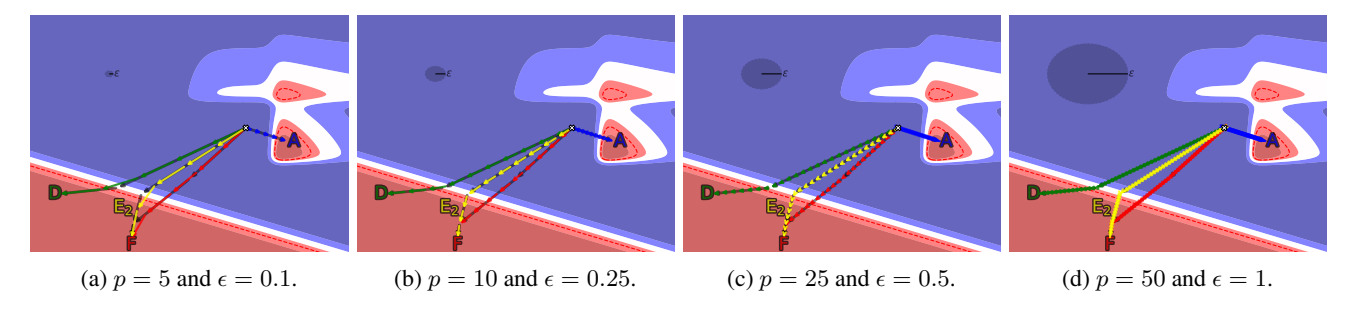


Figure 2: Demonstration of how the number of vectors p into which a path is split and the branching threshold ϵ affect counterfactual trajectories and branching points. These parameters must be carefully selected, which may require domain knowledge and familiarity with the underlying data; e.g., if $\epsilon \ge 1$, paths E_2 and F are not considered to diverge at any point.

Algorithm 1 Split counterfactual path Z into p vectors.

```
Input: counterfactual path Z \in \mathbb{R}^{m \times n}; number of parti-
      tions p \in \mathbb{Z}^+.
    Output: counterfactual path \bar{Z} \in \mathbb{R}^{m \times p} with p steps.
       \textbf{for} \ j \leftarrow 1; \quad j \leftarrow j+1; \quad j \leq p \ \textbf{do} 
          \beta \leftarrow \frac{j}{n}c_L(Z) // split path's total length
 3
          for i \leftarrow 1; i \leftarrow i + 1; i < n do
 4
              if \beta < 0 then
 5
 6
              else if 0 \le \beta \le \|z_i\|_2 then \tau \leftarrow \tau + \frac{\beta}{\|z_i\|_2} z_i
 7
 8
 9
10
                  \tau \leftarrow \tau + z_i
11
              \beta \leftarrow \beta - \|z_i\|_2
12
          end for
13
14
           \bar{z}_j \leftarrow \tau
15
      end for
```

3.2. Identifying Branching Points

We can calculate the proximity between two counterfactual paths $\bar{Z}^{[a]}, \bar{Z}^{[b]} \in \mathbb{R}^{m \times p}$ at all points along $\bar{Z}^{[a]}$, therefore find the location of their divergence. To this end, we compute the minimum distance between the path $\bar{Z}^{[b]}$ and the i^{th} point $\bar{z}^{[a]}_i$ on the path $\bar{Z}^{[a]}$:

$$\bar{z}_i^{[a|b]} = d_S(\bar{Z}^{[b]} - z_i^{[a]} \mathbf{1}_p^T)$$

where

$$d_S(Z) = \min_{1 \le j \le p} ||z_j||_2 = \min_{1 \le j \le p} \sqrt{\sum_{i=1}^m |z_{i,j}|^2}$$

and $\mathbf{1}_p^T = [1 \cdots 1]$ such that $|\mathbf{1}_p| = p$. Next, we define a branching threshold $\epsilon > 0$ such that two paths are considered to have separated at a divergence point $1 \leq p^* \leq p$ if $\bar{z}_i^{[a|b]} \leq \epsilon$ for $1 \leq i < p^* - 1$ but $\bar{z}_i^{[a|b]} > \epsilon$ at $i = p^*$.

Algorithm 2 Identify branching point p^* .

```
Input: counterfactual paths \bar{Z}^{[a]}, \bar{Z}^{[b]} \in \mathbb{R}^{m \times n}; branching threshold \epsilon > 0.

Output: divergence point p^{\star}.

1 for i \leftarrow 1; i \leftarrow i+1; i \leq n do

2 if \bar{z}_i^{[a|b]} > \epsilon then

3 p^{\star} \leftarrow i

4 break

5 end if

6 end for
```

We can then denote the proportion along the journey $\bar{Z}^{[a]}$ before it branches away from $\bar{Z}^{[b]}$ as $\frac{p^*-1}{p}$. This procedure is captured by Algorithm 2 and demonstrated in Figure 2.

3.3. Direction Differences Between Paths

After normalising two counterfactual paths (using Algorithm 1) to have the same number of steps, i.e., $\bar{Z}^{[a]}$, $\bar{Z}^{[b]} \in \mathbb{R}^{m \times p}$, we can compute direction differences between them. One suitable metric is the Frobenius norm

$$s_F(\bar{Z}^{[a]}, \bar{Z}^{[b]}) = \|\mathbf{1}_p w^T \odot (\bar{Z}^{[a]} - \bar{Z}^{[b]})\|_F$$
$$= \sqrt{\sum_{i=1}^m \sum_{j=1}^p \left(w_j(\bar{z}_{i,j}^{[a]} - \bar{z}_{i,j}^{[b]})\right)^2}$$

applied to the weighted difference between the counterfactual journeys, where the weight vector w with |w|=p is as outlined in Section 2.1 and

$$\mathbf{1}_p w^T = \begin{bmatrix} w_1 & \cdots & w_p \\ \vdots & \ddots & \vdots \\ w_1 & \cdots & w_n \end{bmatrix} = \begin{bmatrix} w^T \\ \vdots \\ w^T \end{bmatrix}.$$

Therefore,

$$\begin{split} s_F(\bar{Z}^{[a]},\bar{Z}^{[b]}) &= 0 \implies \bar{Z}^{[a]} \equiv \bar{Z}^{[b]} \\ &\implies \bar{z}_{i,j}^{[a]} = \bar{z}_{i,j}^{[b]} \quad \forall i \; \forall j \; . \end{split}$$

Alternatively, we can use the Euclidean distance such that

$$s_{E}(\bar{Z}^{[a]}, \bar{Z}^{[b]}) = \sum_{j=1}^{p} w_{i} \|\bar{z}_{i,j}^{[a]} - \bar{z}_{i,j}^{[b]}\|_{2}$$
$$= \sum_{j=1}^{p} w_{i} \sqrt{\sum_{i=1}^{m} (\bar{z}_{i,j}^{[a]} - \bar{z}_{i,j}^{[b]})^{2}}.$$

4. Directed Graph Interpretation

Enacting changes to one's situation to achieve the desired outcome is an inherently continuous and incremental process [Barocas et al., 2020]. Given the extended period of time it can span, this process may fail or be abandoned, e.g., due to an unexpected change in circumstances, thus it may require devising alternative paths to the envisaged outcome. However, some of the actions taken thus far may make the adaptation to the new situation difficult or even impossible, prompting us to consider the loss of opportunity captured by counterfactual path branching, in addition to the overall length of the journey. Explanatory multiverse extends the concept of counterfactual paths by accounting for uni-directional changes of features that reflect their monotonicity (as well as immutability) and recognising feature tweaks that cannot be undone; it also models counterfactual path branching. Our directed graph implementation builds upon FACE [Poyiadzi et al., 2020] – see Algorithm 3; specifically, we extend its k-nearest neighbours (k-NN) approach that generates counterfactuals with the shortest path algorithm [Dijkstra, 2022].

4.1. Branching

Let r_i denote the *branching factor* of a node v_i , and $r_{i,j}$ be the branching factor of a path $E_{i,j}$ between nodes v_i and v_j consisting of p steps. r_i can be defined as the *average of the shortest distance* to each instance of the counterfactual class – or all alternative classes for multi-class classification – for node v_i ; its formulation depends on the data set and problem domain (a specific example is provided in Section 4.2). The number of points to consider can be reduced by introducing diversity criteria, e.g., by comparing (absolute) feature difference, thus considering only a few representative counterfactuals. $r_{i,j}$ is defined as the average of individual branching factors r_n corresponding to vertices v_n that are travelled through when following the edges $e_{n,n+1}$ of the counterfactual path $E_{i,j}$, and computed like so:

$$r_{i,j} = \frac{1}{p-2} \sum_{n=1}^{p-1} r_n .$$

The first and last nodes are excluded since the former is shared among all the paths and we stop exploring beyond the latter. To account for choice complexity, we can introduce a Algorithm 3 Build graph-based explanatory multiverse.

Input: data X; probabilistic model f; instance to be explained \mathring{x} ; neighbours number k; counterfactual classification threshold t.

Output: directed data graph G = (V, E); candidate counterfactuals \check{X} ; branching factor of paths R.

```
for every pair (x_i, x_j) \in X do // build graph
         d_{i,j} \leftarrow s(x_i, x_j) // \text{ compute distance}
         if d_{i,j} \neq 0 then
 3
            e_{i,j} \leftarrow \omega(d_{i,j}) // transform into weight
 4
 5
 6 end for
    V \leftarrow X
 8 E \leftarrow prune(E, k) // \text{ keep } k\text{-NN for each node}
10 for x_i \in X do
         if f(x_i) \ge t then
11
            \check{X} \leftarrow \check{X} \cup i
12
            E_{j,i} \leftarrow dijkstra(G, \mathring{x}_j, x_i) \; / / \; \text{shortest path} \\ r_{j,i} \leftarrow branching(G, E_{j,i})
13
15
16
    end for
```

discount factor $\gamma \in \mathbb{R}$ that allows us to reward $(\gamma > 1)$ or penalise $(\gamma < 1)$ branching in the early stages of a path:

$$r_{i,j} = \frac{1}{p-2} \sum_{n=1}^{p-1} \gamma^{n-1} r_n$$
.

4.2. Constraining Feature Changes

For many data domains, the strict directionality of change assumption imposed upon features may be too restrictive, as is the case for our next example – path-based counterfactual explanations for the MNIST data set of handwritten digits [LeCun, 1998]. Assuming that transitions between digits can only add pixels yields no viable paths, therefore we relax this constraint such that removing pixels is λ times more difficult than adding them, where $\lambda \in \mathbb{R}^+$ is a penalty term, with the corresponding distance between two nodes v_a and v_b defined like so:

$$s_{\lambda}(v_a, v_b) = \sqrt{\sum_{i=1}^{m} (\phi(v_{a,i}, v_{b,i})(v_{a,i} - v_{b,i}))^2},$$

where $v_{a,i}$ is the i^{th} feature of the instance x_a represented by the node v_a and

$$\phi(v_{a,i}, v_{b,i}) = \begin{cases} -\lambda & \text{if } v_{a,i} - v_{b,i} < 0 \\ 1 & \text{if } v_{a,i} - v_{b,i} \ge 0 \end{cases}.$$

We apply Algorithm 3 with k=20 using this distance function for $\lambda=1.1$. Figure 3 shows example counterfactual

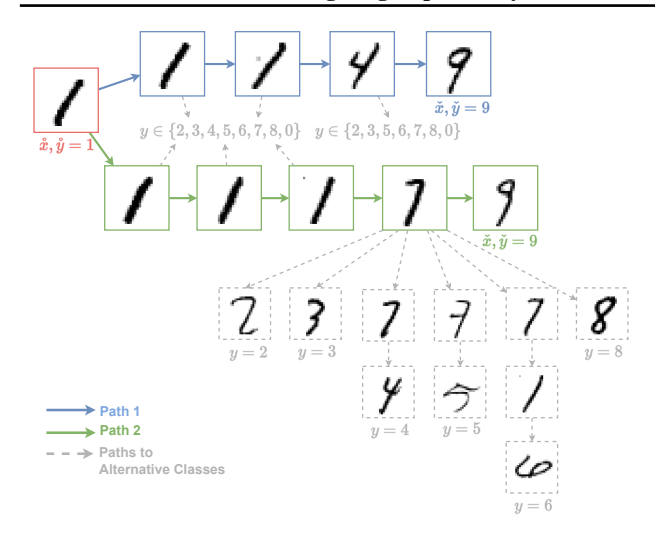


Figure 3: Example counterfactual journeys identified in the MNIST data set of handwritten digits. Paths 1 (blue) and 2 (green) explain an instance \mathring{x} classified as $\mathring{y}=1$ for the counterfactual class $\check{y}=9$. Paths leading to alternative classification outcomes are also possible (shown in grey). Path 1 is shorter than Path 2 at the expense of explainees' agency – which is reflected in its smaller branching factor – therefore switching to alternative paths leading to different classes is easier, i.e., less costly in terms of distance.

paths starting at $f(\mathring{x}) = 1$ and terminating at $f(\check{x}) = 9$. The branching factor of a node v_i representing a digit is computed as $r_i = -log(c(v_i))$ for

$$c(v_i) = \frac{1}{|Y'|} \sum_{y \in Y'} \sum_{e_{a,b} \in E_{i,j}} s_\lambda(v_a, v_b) \quad \text{s.t.} \quad f(v_j) = y \;,$$

where $Y' \equiv \mathcal{Y} \setminus (f(v_i), \mathring{y}, \widecheck{y})$, excluding the class of the factual and counterfactual instances as well as $f(v_i)$ if v_i is an intermediate step, and $E_{i,j}$ is the shortest path from v_i to nodes v_j that represent counterfactual instances, i.e., $f(v_j) \in Y'$.

5. Discussion

Explanatory multiverse is a novel conceptualisation of stepbased counterfactual explanations (overviewed in Section 1) that inherits all of their desired, spatially-unaware, properties and extends them with a collection of spatially-aware desiderata that take advantage of the geometry of counterfactual paths (covered in Section 2.2). Despite being overlooked in the technical literature, such a view on counterfactual reasoning and explainability is largely consistent with their philosophical and psychological account [Kahneman, 2014]. Lewis' [1973] notion of *possible-worlds*, of which the real world is just one and with some being closer to reality (more realistic) than others [Kahneman & Varey, 1990], is akin to explanatory multiverse we propose in this paper. They both exhibit spatial and temporal contiguity, thus support and better align with *mental simulation*, which is a form of automatic and elaborative (counterfactual) thinking. This process spans continuum rather than a typology and allows to imagine congruent links between two possible states of the world, e.g., factual and counterfactual, by unfolding a sequence of events connecting them.

Navigating the nexus of (hypothetical) possibilities through the (technical) proxy of explanatory multiverse enables structured - and possibly guided - exploration, comparison and reasoning over (remote branches of) counterfactual explanations. By accounting for the spatial and temporal aspects of their paths – such as affinity, branching, divergence and convergence – we construct an explainability framework capable of modelling a perceptual distance between counterfactual trajectories. For example, it allows us to consider the fact that people first tend to undo the changes enacted at the beginning and, once committed, they fall prey to the sunk cost fallacy – a tendency to continue an endeavour after an initial effort [Arkes & Blumer, 1985]. To the best of our knowledge, we are the first to model the geometry of explanations, thus better align ML interpretability with modes of counterfactual thinking found in humans.

Explanatory multiverse also advances the human-centred explainability agenda on multiple fronts. It comes with an inherent heuristic to deal with counterfactual multiplicity by recognising their spatial (dis)similarity, thus reducing the cognitive load required of explainees. By lowering the choice complexity when deciding on actions to take while navigating and traversing step-based counterfactual paths, explanatory multiverse better aligns this process with iterative and interactive, dialogue-based, conversational explainability – a process that is second nature to humans [Miller, 2019; Keenan & Sokol, 2023]. Given the ability to consider the general direction of representative counterfactual paths instead of their specific instantiations (which may be overwhelming due to their quantity and lack of meaningful differentiation), our conceptualisation is compatible with both the well-established justification as well as the more recent decision-support paradigms of explainable ML [Miller, 2023]. An additional benefit of explanatory multiverse is its ability to uncover disparity in access to counterfactual recourse – a fairness perspective; some individuals may only be offered a limited set of explanations, or none at all, if they belong to remote clusters of points, e.g., portraying a protected group that is underrepresented in our data.

The three preliminary desiderata outlined in Section 2.2 are general enough to encompass most applications of explanatory multiverse, nonetheless they are far from exhaustive; we envisage identifying more properties as we explore this concept further and apply it to specific problems. Doing so will allow us to learn about their various trade-offs, espe-

cially since we expect different data domains and modelling problems to prioritise distinct desiderata. With the current set of properties, for example, one may prioritise delayed branching, which incurs small loss of opportunity early on but a large one at later stages, thus initially preserving high agency. Similarly, a small loss of opportunity early on can be accepted to facilitate delayed branching, hence reduce overall choice complexity at the expense of agency. If, in contrast, early branching is desired – for example, one prefers a medical diagnosis route with fewer required tests - this will result in a large loss of opportunity at the beginning, thus lower agency. Additionally, certain paths may be easier to follow, i.e., preferred, due to domain-specific properties, e.g., a non-invasive medical examination, whereas others may require crossing points of no return, i.e., enacting changes that cannot be (easily) undone. Forgoing naïve optimisation for the shortest path and sacrificing the distance travelled for a deliberate detour can benefit explainees on multiple levels as outlined above. Some of these considerations can be communicated through intuitive visualisations, making them more accessible (to a lay audience); for example, we may plot the number of enacted changes against the proportion of counterfactual recourse opportunities that remain available at any given point.

In view of the promising results offered by our initial experiments, streamlining and extending both of our approaches as well as implementing their variations (e.g., vector paths can also be based on gradient methods) are the next steps, which will allow us to transition away from toy examples and apply our tools to real-life data sets. The vector interpretation of explanatory multiverse is best suited for continuous spaces for which we have a sizeable and representative sample of data. The (directed) graph perspective, on the other hand, is more appropriate for sparse data sets with discrete attributes. Both solutions are inherently compatible with multi-class counterfactuals [Sokol & Flach, 2020b] – refer back to the MNIST example shown in Figure 3 – which offer a nuanced and comprehensive explanatory perspective. Note that an action may have multiple distinct consequences: make certain outcomes more likely (or simply possible), others less likely (or even impossible), or both at the same time; therefore, depending on the point of view, each step taken by an explainee can be interpreted as a negative or positive (counterfactual) explanation. Our solutions also facilitate retrospective explanations that allow us to (mentally) backtrack steps leading to the current situation (in contrast to prospective explanations that prescribe actionable insights), thus answering questions such as: "How did I end up here?"

6. Conclusion and Future Work

In this paper we introduced *explanatory multiverse*: a novel conceptualisation of counterfactual explainability that takes

advantage of *geometrical relation* – affinity, branching, divergence and convergence – between paths representing the steps leading from factual to counterfactual data points. Our approach better aligns such explanations with human needs and expectations by distilling informative, intuitive and actionable insights from, otherwise overwhelming, *counterfactual multiplicity*; explanatory multiverse is also compatible with iterative and interactive explanatory protocols, which are one of the tenets of human-centred explainability.

To guide the retrieval of high-quality explanations, we formalised three spatially-aware desiderata: agency, loss of opportunity and choice complexity; nonetheless, this is just a preliminary and non-exhaustive set of properties, which we expect to expand as we explore explanatory multiverse further and apply it to specific data domains. In addition to foundational and theoretical contributions, we also proposed and implemented two algorithms - one based on vector spaces and the other on (directed) graphs – which we evaluated across two toy examples – a synthetic twodimensional tabular data set and the MNIST hand-written digits respectively - to demonstrate the capabilities of our approach. Our methods, the implementation of which is available on GitHub to promote reproducibility, are built upon state-of-the-art, step-based counterfactual explainers, such as algorithmic recourse, therefore they come equipped with all the desired, spatially-unaware properties.

By introducing and formalising explanatory multiverse, we laid the foundation necessary for further exploration of this concept. In addition to advancing the two methods outlined in this paper, in future work we will study building dynamical systems, phase spaces and vector fields from (partial) sequences of observations to capture divergence and verticity within explanatory multiverse, which appears suitable for medical data such as electronic health records. We will also look into explanation representativeness - i.e., identifying and grouping counterfactuals that are the most diverse and least alike - given that it is central to navigating the geometry of counterfactual paths yet largely under-explored. Discovering (dis)similarity of counterfactuals can streamline the exploration of explanatory multiverse, whether with graphs or vectors, helping to identify pockets of highly attractive and inaccessible explanations; understanding these dependencies is also important given their fairness ramifications as some individuals may only have limited options for explanatory recourse.

Acknowledgements

This research was conducted by the ARC Centre of Excellence for Automated Decision-Making and Society (project number CE200100005), funded by the Australian Government through the Australian Research Council.

Authors' Contributions

Conceptualisation: Kacper Sokol (lead investigator), Edward Small, Yueqing Xuan. Methodology: Kacper Sokol (explanatory multiverse), Edward Small (vector-based approach), Yueqing Xuan (graph-based approach). Code development: Edward Small (vector-based approach), Yueqing Xuan (graph-based approach). Writing: Kacper Sokol (explanatory multiverse), Edward Small (vector-based approach), Yueqing Xuan (graph-based approach). Review and editing: Kacper Sokol.

References

- Arkes, H. R. and Blumer, C. The psychology of sunk cost. *Organizational behavior and human decision processes*, 35(1):124–140, 1985.
- Barocas, S., Selbst, A. D., and Raghavan, M. The hidden assumptions behind counterfactual explanations and principal reasons. In *Proceedings of the 2020 conference on fairness, accountability, and transparency*, pp. 80–89, 2020.
- Dijkstra, E. W. A note on two problems in connexion with graphs. In *Edsger Wybe Dijkstra: His Life, Work, and Legacy*, pp. 287–290. 2022.
- Downs, M., Chu, J. L., Yacoby, Y., Doshi-Velez, F., and Pan, W. CRUDS: Counterfactual recourse using disentangled subspaces. *ICML WHI*, 2020:1–23, 2020.
- Förster, M., Hühn, P., Klier, M., and Kluge, K. Capturing users' reality: A novel approach to generate coherent counterfactual explanations. 2021.
- Kahneman, D. Varieties of counterfactual thinking. In *What might have been*, pp. 387–408. Psychology Press, 2014.
- Kahneman, D. and Varey, C. A. Propensities and counterfactuals: The loser that almost won. *Journal of Personality and Social Psychology*, 59(6):1101, 1990.
- Karimi, A., Schölkopf, B., and Valera, I. Algorithmic recourse: From counterfactual explanations to interventions. In *Proceedings of the 2021 ACM conference on fairness*, accountability, and transparency, pp. 353–362, 2021.
- Keane, M. T. and Smyth, B. Good counterfactuals and where to find them: A case-based technique for generating counterfactuals for explainable AI (XAI). In *Case-Based Reasoning Research and Development: 28th International Conference, ICCBR 2020, Salamanca, Spain, June 8–12, 2020, Proceedings 28*, pp. 163–178. Springer, 2020.
- Keane, M. T., Kenny, E. M., Delaney, E., and Smyth, B. If only we had better counterfactual explanations: Five key

- deficits to rectify in the evaluation of counterfactual XAI techniques. In *IJCAI*, pp. 4466–4474, 2021.
- Keenan, B. and Sokol, K. Mind the gap! Bridging explainable artificial intelligence and human understanding with Luhmann's functional theory of communication. *arXiv* preprint arXiv:2302.03460, 2023.
- LeCun, Y. The MNIST database of handwritten digits. http://yann.lecun.com/exdb/mnist/, 1998.
- Lewis, D. *Counterfactuals*. Harvard University Press, Cambridge, Massachusetts, 1973.
- Miller, T. Explanation in artificial intelligence: Insights from the social sciences. *Artificial Intelligence*, 267:1–38, 2019.
- Miller, T. Explainable AI is dead, long live explainable AI! Hypothesis-driven decision support. In *Proceedings* of the 2023 conference on fairness, accountability, and transparency, 2023.
- Mothilal, R. K., Sharma, A., and Tan, C. Explaining machine learning classifiers through diverse counterfactual explanations. In *Proceedings of the 2020 conference on fairness, accountability, and transparency*, pp. 607–617, 2020.
- Pawelczyk, M., Broelemann, K., and Kasneci, G. Learning model-agnostic counterfactual explanations for tabular data. In *Proceedings of the 2020 web conference*, pp. 3126–3132, 2020.
- Poyiadzi, R., Sokol, K., Santos-Rodriguez, R., De Bie, T., and Flach, P. FACE: Feasible and actionable counterfactual explanations. In *Proceedings of the AAAI/ACM Conference on AI, Ethics, and Society*, pp. 344–350, 2020.
- Romashov, P., Gjoreski, M., Sokol, K., Martinez, M. V., and Langheinrich, M. BayCon: Model-agnostic Bayesian counterfactual generator. In *IJCAI*, pp. 740–746, 2022.
- Russell, C. Efficient search for diverse coherent explanations. In *Proceedings of the 2019 conference on fairness, accountability, and transparency*, pp. 20–28, 2019.
- Small, E., Xuan, Y., Hettiachchi, D., and Sokol, K. Helpful, misleading or confusing: How humans perceive fundamental building blocks of artificial intelligence explanations. ACM CHI 2023 Workshop on Human-Centered Explainable AI (HCXAI), 2023.
- Sokol, K. and Flach, P. Glass-Box: Explaining AI decisions with counterfactual statements through conversation with a voice-enabled virtual assistant. In *IJCAI*, pp. 5868–5870, 2018.

- Sokol, K. and Flach, P. Explainability fact sheets: A framework for systematic assessment of explainable approaches. In *Proceedings of the 2020 conference on fairness, accountability, and transparency*, pp. 56–67, 2020a
- Sokol, K. and Flach, P. LIMEtree: Consistent and faithful surrogate explanations of multiple classes. *arXiv* preprint *arXiv*:2005.01427, 2020b.
- Sokol, K. and Flach, P. One explanation does not fit all. *KI-Künstliche Intelligenz*, pp. 1–16, 2020c.
- Tolomei, G., Silvestri, F., Haines, A., and Lalmas, M. Interpretable predictions of tree-based ensembles via actionable feature tweaking. In *Proceedings of the 23rd ACM SIGKDD international conference on knowledge discovery and data mining*, pp. 465–474, 2017.

- Ustun, B., Spangher, A., and Liu, Y. Actionable recourse in linear classification. In *Proceedings of the 2019 conference on fairness, accountability, and transparency*, pp. 10–19, 2019.
- van Looveren, A. and Klaise, J. Interpretable counterfactual explanations guided by prototypes. In *Machine Learning and Knowledge Discovery in Databases. Research Track: European Conference, ECML PKDD 2021, Bilbao, Spain, September 13–17, 2021, Proceedings, Part II 21*, pp. 650–665. Springer, 2021.
- Wachter, S., Mittelstadt, B., and Russell, C. Counterfactual explanations without opening the black box: Automated decisions and the GPDR. *Harv. JL & Tech.*, 31:841, 2017.